Efficient reconstruction of multiphase morphologies from correlation functions

M. G. Rozman* and Marcel Utz†
Institute of Materials Science and Department of Physics, University of Connecticut, Storrs, Connecticut 06269
(Received 11 December 2000; published 15 May 2001)

A highly efficient algorithm for the reconstruction of microstructures of heterogeneous media from spatial correlation functions is presented. Since many experimental techniques yield two-point correlation functions, the restoration of heterogeneous structures, such as composites, porous materials, microemulsions, ceramics, or polymer blends, is an inverse problem of fundamental importance. Similar to previously proposed algorithms, the new method relies on Monte Carlo optimization, representing the microstructure on a discrete grid. An efficient way to update the correlation functions after local changes to the structure is introduced. In addition, the rate of convergence is substantially enhanced by selective Monte Carlo moves at interfaces. Speedups over prior methods of more than two orders of magnitude are thus achieved. Moreover, an improved minimization protocol leads to additional gains. The algorithm is ideally suited for implementation on parallel computers. The increase in efficiency brings new classes of problems within the realm of the tractable, notably those involving several different structural length scales and/or components.

DOI: 10.1103/PhysRevE.63.066701 PACS number(s): 02.70.−c, 61.43.Bn, 05.10.Ln, 81.07.−b

I. INTRODUCTION

Heterogeneous media, such as composites, porous materials, or polymer blends, often exhibit complex microstructures. While many important characterization techniques provide morphological information in the form of spatial correlation functions, a real-space microstructural model is needed for understanding and predicting material properties. Therefore, finding microstructures consistent with a given correlation function is important for both materials science and technology.

Several different approaches have been taken to solve this inverse problem [1–15]. A scheme originally proposed by Cahn [1] associates interfaces between two phases with isosurfaces of a correlated random Gaussian field; a region of space is attributed to a phase according to whether the value of a Gaussian random variable is within a specified range. This method was originally devised for the description of phase separation by spinodal decomposition [1]. It has been applied to the reconstruction of two phase systems by Quiblier [2], and further significant advances in its mathematical structure have been reported since [3–8]. Adler [9] and Levitz [10] have evaluated the method for different types of geometrical disorder and compared it to experimental results on porous media. Recently, the method has been applied to the analysis of scattering data from block copolymers and microemulsions [16,17].

However, the random Gaussian field method suffers from several inherent limitations. The Gaussian character of the field is essential, making it is impossible to generalize the method to other statistics. The implications of this in terms of limitations imposed on the phase geometries that can be generated are not presently fully understood. Even more importantly, it is difficult to generalize the approach to systems with more than two phases [18].

Recently, Torquato and co-workers [11–13] have proposed a stochastic reconstruction procedure based on discretization of the spatial structure on a grid, each pixel of which is attributed to a single phase. The method departs from an arbitrary configuration and then minimizes the discrepancy between the actual and target correlation functions by simulated annealing.

The discrete stochastic minimization approach is attractive due to its generality and flexibility. No restrictions are imposed on microstructures and there is no limit, in principle, to the number of different phases in the system. In addition, structural information in forms other than correlation functions can be taken into account in the restoration process [11].

The main disadvantage of the method lies in its high computational cost. In this discretized form, the reconstruction problem is related to the search for a ground state of a spin system with long-range multispin interactions, since the target correlation function couples the state of pixels at both small and large separations on the grid. Linear chains of spins with long-range interactions have been studied extensively over the past decade [19–22], and have acquired a reputation to be among the hardest discrete minimization problems known [22].

Due to this complex nature of the minimization problem, a large number of Monte Carlo steps is required to achieve convergence. In addition, the recalculation of the correlation function at every attempted step is an expensive operation [11]. To date, the most efficient version of the algorithm is based on the discrete fast Fourier transform (FFT), requiring $O(N \ln N+N)$ operations, where N is the number of pixels on the grid [13].

This computational demand severely limits the applicability of the method. When high digital resolution is important, for instance, in systems that contain several different structural length scales, it can only be applied with difficulty. In order to improve performance, it has been proposed to evaluate the discrepancy between the target and actual correlation

*On leave from the Institute of Physics, Tartu University, Tartu, Estonia. URL: http://giotto.ims.uconn.edu/~rozman/
†Electronic address:
marcel.utz@uconn.edu, http://giotto.ims.uconn.edu/~mutz/

function only along selected spatial directions [11]. While significantly reducing the computational load, this has been shown to lead to the undesirable generation of structures with lower symmetry than the target correlation function [13,14].

In the present contribution, we propose a discrete minimization algorithm for restoration that avoids these shortcomings. The new algorithm uses a method to update the correlation function much faster than the FFT, requiring only $O(N)$ operations. This is possible by reusing the correlation function from the previous configuration, rather than recomputing it from scratch at every step. In addition, candidate pixels for the Monte Carlo moves are chosen exclusively at phase boundaries, and a minimization method different from the traditional simulated annealing protocol is used. It will be shown that these improvements together lead to speedups of more than three orders of magnitude. In addition, the method is easily implemented on parallel computer architectures.

The rest of the paper is organized as follows. Section II introduces the reconstruction algorithm in detail. In Sec. III, the method is applied to several two- and three-phase systems. The implementation of the new algorithm on parallel computer architectures is discussed in Sec. IV. Finally, conclusions are drawn in Sec. V. In the Appendix the update procedure is described in a form suitable for programming, and some implementation details important for algorithm performance are discussed.

II. COMPUTATIONAL METHODS

A. Mathematical formulation of the reconstruction problem

In order to numerically describe a random medium it is necessary to introduce a finite cell subject to periodic continuation conditions such that an infinite medium is composed of periodic ''images'' of the fundamental cell. We denote the cell symbolically by $\mathcal{V}$ and spatial integration over the cell is represented by $\int_{\mathcal{V}} d\mathbf{r} \ldots$. The cell volume is then

$$V=\int_{\mathcal{V}} d\mathbf{r}.$$

The microstructure of a material consisting of n components is completely described by the local densities $\rho_i(\mathbf{r})$, $i=1 \ldots n$. By definition, the ρ_i are positive quantities. The average concentration of component i can be written as

$$\phi_i=\langle \rho_i \rangle = \frac{1}{V}\int_{\mathcal{V}} d\mathbf{r}\rho_i(\mathbf{r}). \tag{1}$$

The angular brackets in Eq. (1) denote the ensemble average, which can be replaced by the volume average,

$$\langle \ldots \rangle \equiv \frac{1}{V}\int_{\mathcal{V}} d\mathbf{r} \ldots$$

if the system is stationary and macroscopically homogeneous.

The two-point correlation functions $G_{ij}(\mathbf{r})$ are defined as

$$G_{ij}(\mathbf{r})=\langle \rho_i(0)\rho_j(\mathbf{r}) \rangle \tag{2}$$

$$=\frac{1}{V}\int_{\mathcal{V}} d\mathbf{r}' \rho_i(\mathbf{r}')\rho_j(\mathbf{r}+\mathbf{r}'). \tag{3}$$

The problem under study here is to find a set of density functions $\{\rho_i(\mathbf{r})\}$ that are consistent with a given set of correlation functions $\{G^t_{ij}(\mathbf{r})\}$ to within a specified precision. As is well known, this inverse problem is ill posed in general [11]. Therefore any practical algorithm selects a microstructure from the manifold of possible solutions, minimizing the discrepancy Δ between the configuration $\{\rho_i(\mathbf{r})\}$ and a given set of target correlation functions $\{G^t_{ij}(\mathbf{r})\}$, where Δ is defined as

$$\Delta=\sum_{ij} \int_{\mathcal{V}} d\mathbf{r} |G_{ij}(\mathbf{r})-G^t_{ij}(\mathbf{r})|. \tag{4}$$

Starting from a given configuration, a new one can be obtained by applying a series of local changes to the densities ρ_i. The next section discusses the response of the correlation functions to such local perturbations.

B. Update of correlation functions after local perturbations

As outlined in the Introduction, previously proposed algorithms to reconstruct discrete two-phase systems [11–15] are based on Monte Carlo type minimization of the discrepancy Δ. Randomly chosen local changes in the discretized density are accepted or rejected using a simulated annealing protocol. The change in the discrepancy Δ must be computed for each attempted Monte Carlo step in order to decide whether it should be accepted or rejected. To this end, the correlation function has been recalculated completely from scratch after every attempted step [13].

Closer analysis, however, reveals that the response of the correlation function to a *local* change in density can be obtained in a computationally much less costly way if the correlation function *before* the change is known.

In order to illustrate the idea, it is sufficient to discuss the response of the autocorrelation function $G(\mathbf{r})$ to a local perturbation in the density; the case of cross-correlation functions is completely analogous. The simplest local change in the density can be represented as

$$\rho^n(\mathbf{r})=\rho^o(\mathbf{r})+a\,\delta(\mathbf{r}-\mathbf{r_1}), \tag{5}$$

where ρ^o and ρ^n are the density functions before and after the perturbation. a is the magnitude of the change and $\delta(\mathbf{r})$ denotes Dirac's delta function [23]. Using the definition of the correlation function, we obtain

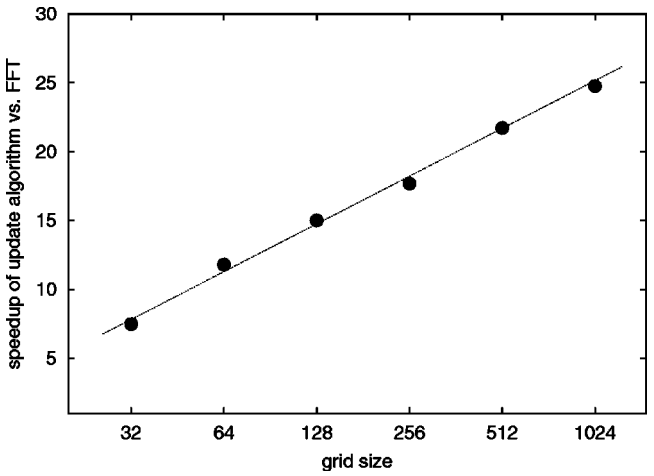

FIG. 1. Speedup of the update algorithm with respect to FFT vs linear size of the grid. The line $y=5\ln x-9.5$ is provided as a guide to the eye.

$$G^n(\mathbf{r})=\frac{1}{V}\int_{\mathcal{V}} d\mathbf{r}'\,\rho^n(\mathbf{r}')\rho^n(\mathbf{r}+\mathbf{r}') \tag{6}$$

$$=\frac{1}{V}\int_{\mathcal{V}} d\mathbf{r}'[\rho^o(\mathbf{r}')+a\,\delta(\mathbf{r}'-\mathbf{r_1})][\rho^o(\mathbf{r}+\mathbf{r}') + a\,\delta(\mathbf{r}+\mathbf{r}'-\mathbf{r_1})] \tag{7}$$

$$=\frac{1}{V}\int_{\mathcal{V}} d\mathbf{r}'[\rho^o(\mathbf{r}')\rho^o(\mathbf{r}+\mathbf{r}')+a\rho^o(\mathbf{r}')\,\delta(\mathbf{r}+\mathbf{r}'-\mathbf{r_1}) + a\rho^o(\mathbf{r}+\mathbf{r}')\,\delta(\mathbf{r}'-\mathbf{r_1})+a^2\delta(\mathbf{r}'-\mathbf{r_1})\,\delta(\mathbf{r}+\mathbf{r}'-\mathbf{r_1})] \tag{8}$$

$$=G^o(\mathbf{r})+a[\rho^o(\mathbf{r}-\mathbf{r_1})+\rho^o(\mathbf{r}+\mathbf{r_1})]+a^2\delta(\mathbf{r}). \tag{9}$$

Hence, the updated correlation function $G^n(\mathbf{r})$ can essentially be found from the ''old'' one $G^o(\mathbf{r})$ by a simple addition of the shifted density function. If this is done on a discrete grid of N cells, it requires only $O(N)$ operations as opposed to $O(N\ln N+N)$ if the fast Fourier transform is used. In practice, this translates to a speedup by one to two orders of magnitude. Figure 1 shows the speedup factor between Eq. (9) and the fast Fourier transform [24] for a single Monte Carlo step (exchange of the contents of two pixels on a two-dimensional grid) as a function of grid size. The update scheme is not restricted to two-point correlation functions. It can be generalized to higher order correlation functions in a straightforward manner.

The last term in Eq. (9), which does not depend on $\mathbf{r_1}$, reflects the change in the average concentration caused by the perturbation,

$$\phi^n=\frac{1}{V}\int_{\mathcal{V}} d\mathbf{r}\rho^n(\mathbf{r})=\phi^o+\frac{a}{V}. \tag{10}$$

The average concentrations can easily be computed from a given set of correlation functions. Hence, it is always possible in practice to depart from a configuration that represents them correctly. It is therefore advantageous to use elementary Monte Carlo steps that conserve the concentrations such as exchanging the contents of two pixels.

In the rest of the paper, we will restrict the discussion to the case of *complete segregation* of the components into separate phases. In this case, it is possible to completely characterize the microstructure in terms of characteristic density functions, which are defined in the following way:

$$\rho_i(\mathbf{r})=\begin{cases}1, & \text{when } \mathbf{r} \text{ is within phase } i\\ 0, & \text{otherwise.}\end{cases} \tag{11}$$

This means that at every location $\mathbf{r}$, exactly one of the densities $\{\rho_i(\mathbf{r})\}$ is equal to 1, whereas all the others vanish. In this case, the density functions obey the relation

$$\rho_i(\mathbf{r})=\rho_i^2(\mathbf{r}), \tag{12}$$

and the average concentrations ϕ_i adopt the meaning of volume fractions.

We will represent the microstructure inside the periodic cell on an orthogonal grid, each pixel of which will contain exactly one of the i different components. Accordingly discretized formulas for the update of the auto-correlation and cross-correlation functions, which are directly suitable for implementation on a computer, are presented in the Appendix.

C. Restriction to interfacial Monte Carlo moves

For an accurate description of a microstructure on a discrete grid, the size of the pixels must be chosen considerably smaller than the smallest feature size present in the structure. If this condition is fulfilled each phase in the system, whatever its geometrical shape, is composed of a large number of contiguous pixels. In other words, the overwhelming majority of pixels will be completely surrounded by others that contain the same component.

Selecting candidate pixels for Monte Carlo moves completely at random runs counter to this observation. In the vast majority of cases, such moves will generate single, isolated pixels of one phase embedded in another. Eventually, of course, the minimization procedure will remove these artifacts and converge to a compact structure in agreement with the given correlation functions. However, much of the computer time necessary for minimization is used solely to remove such spurious isolated pixels.

This can be remedied by selecting exclusively *interfacial* pixels (which have at least one neighbor that contains a different component) as candidates for an exchange Monte Carlo step. As illustrated in Fig. 3, this substantially increases the rate of convergence. The resulting speedup is most significant in the later stage of reconstruction.

It is important to note that the restriction to interfacial moves does not lead to conservation of the number of interfacial pixels in the system, since a pixel is allowed to have a different number of unlike neighbors before and after a move. Therefore, the method remains *ergodic*, i.e., all configurations possible at the given volume fractions are acces-

sible from any starting configuration.

The selection of interfacial pixels requires some computational effort. In principle, it is possible to keep track of all interfacial pixels in a suitable dynamic data structure. Once established, this list can be continuously kept up to date at marginal cost. However, in all cases studied, the computer time needed per Monte Carlo move is strongly dominated by the update of the correlation functions. Even if the selection is done by repeated random choice until an interfacial pixel is found, the overhead remains negligible.

D. Optimization technique

In addition to the improvements described in the previous sections, we have found that a simpler variant of stochastic minimization than the traditional simulated annealing approach leads to faster convergence in all cases studied. Instead of the conventional Metropolis criterion, our algorithm simply accepts a move if it decreases the discrepancy Δ and rejects it otherwise. This is related to the ''Great Deluge'' algorithm which has been successfully applied to this problem by Cule and Torquato [13]. In the initial stage of minimization, where the discrepancy is large, this leads to a rapid rate of convergence. Eventually, however, when convergence is almost achieved, the acceptance ratio becomes impracticably low. At this stage, we found it advantageous to allow for an ''uphill'' move once in a while. The algorithm presented in this contribution achieves this by accepting a single Monte Carlo move after a specified (large) number of continuous rejections, regardless of the change in the discrepancy it causes.

Whereas the conventional simulated annealing protocol relies on several parameters (number of temperature levels, number of equilibration steps at each level, starting temperature), all of which must be carefully tuned to the problem under study, the method outlined above has only a single one (the number of rejections until an ''uphill'' move is allowed), which is very simple to choose in practice.

III. RESULTS AND DISCUSSION

While the algorithm is completely independent of the number of spatial dimensions, the examples presented in the following are two-dimensional for convenience of visualization.

A. A simple test case

As a simple test, a target autocorrelation function was obtained from the periodic two-phase structure shown in Fig. 2(a). Departing from the initial (random) configuration shown in Fig. 2(b), the target structure becomes already roughly recognizable after about 7000 attempted Monte Carlo moves (2000 accepted steps) [Fig. 2(d)]. After 15 000 attempted moves, the structure is essentially correct, with the exception of a small number of pixels on the phase boundaries [Fig. 2(e)]. Using a number of different initial configurations, random as well as layered, it was verified that the restoration process does not depend on the initial state.

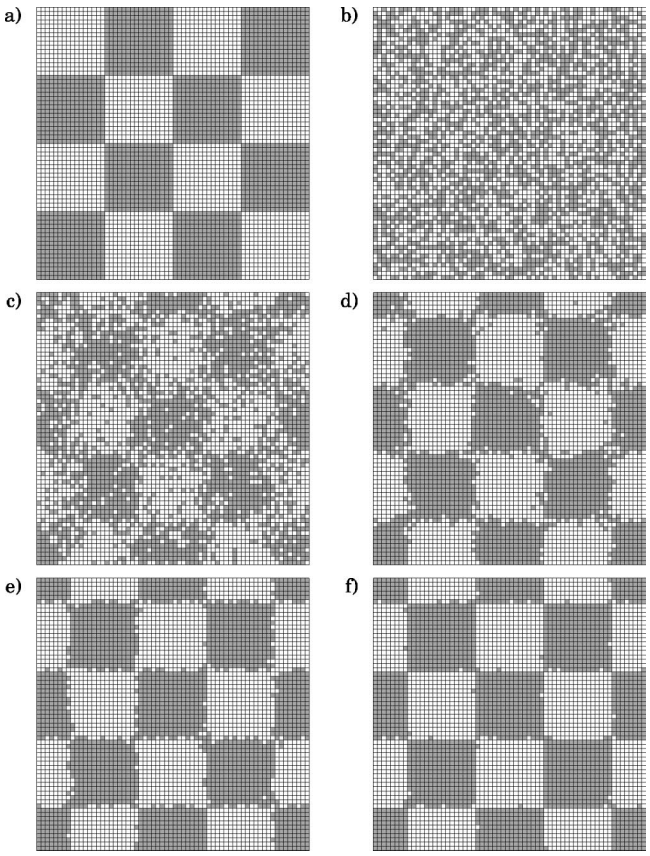

FIG. 2. Simple two-phase test system. (a) Target structure, (b) initial random configuration, (c) configuration after 2706 attempted Monte Carlo moves (1000 accepted steps), (d) configuration after 7132 attempted Monte Carlo moves (2000 accepted steps), (e) configuration after 15 000 attempted Monte Carlo moves (2360 accepted steps), (f) final configuration (150 000 attempted Monte Carlo moves, 2535 accepted steps).

Figure 3 illustrates the convergence behavior of the algorithm. The decrease of the discrepancy, shown in Fig. 3(a), is significantly more rapid if only interfacial Monte Carlo moves are used (solid line) rather than when no such restriction is applied (dashed line). The concentration of interfacial pixels is plotted in Fig. 3(b). Starting at a high value of 0.88 for the random initial structure, interfacial Monte Carlo moves bring it quickly close to the correct value of $\frac{15}{64} \approx 0.234$. As is obvious from the figure, this takes very much longer if candidate pixels are chosen completely at random.

The restriction to interfacial moves leads to two clearly distinct kinetic regimes. First, a rough approximation to the structure is found as shown in Fig. 2(d). This stage is characterized by a rapid decay of the discrepancy and a high acceptance ratio of the Monte Carlo moves.

At some point, the acceptance ratio drops significantly and the convergence slows down. This stage is reached when the concentration of interfacial pixels has roughly converged to the correct value and the target correlation function is already quite well reproduced. After this point, the structure remains essentially unaltered in general appearance but is gradually refined in detail.

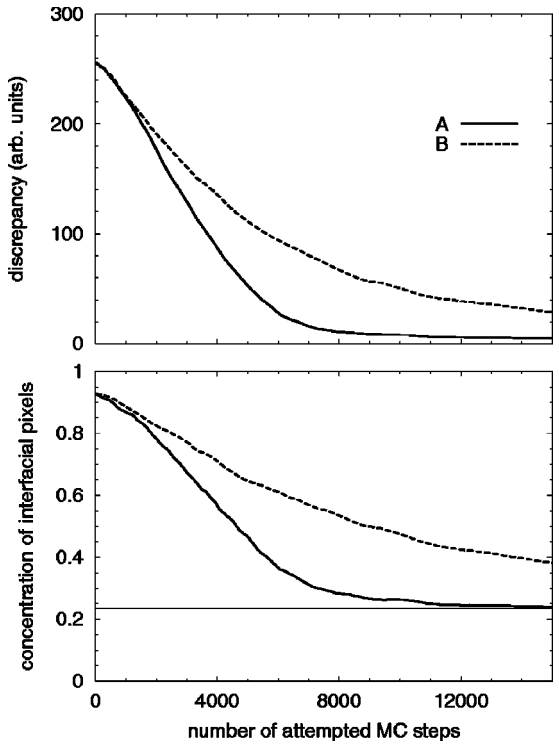

FIG. 3. Convergence of the algorithm for the test structure in Fig. 2. The solid lines correspond to selective Monte Carlo moves using interfacial pixels only, whereas dashed curves were obtained using completely random moves. Top panel: convergence of the discrepancy, bottom panel: convergence of the interfacial pixel concentration. The horizontal line indicates the target value $\frac{15}{64} \approx 0.234$.

B. Construction of two-phase systems

Rather than from a given target configuration, it is also possible to depart from an analytically specified autocorrelation function such as [6,13]

$$G(\mathbf{r}) = \phi^2 + \phi(1-\phi)e^{-r/r_0}\frac{\sin(2\pi r/a_0)}{2\pi r/a_0}, \qquad (13)$$

which applies to a two-component system where ϕ is the volume fraction of phase 1. The parameters r_0 and a_0 control the overall exponential damping and the short-range oscillatory behavior of the correlation function, respectively. In the limit $a_0 \ll r_0$, a_0 determines the short-range structural length scale of the medium. Equation (13) has been used extensively as a benchmark for reconstruction [6,13]. A typical structure calculated using the parameters $\phi = 0.55$, $r_0 = 1.1L$, $a_0 = 0.125L$, where L is the linear size of the cell, is presented in Fig. 4(b).

After about 900 000 accepted Monte Carlo steps the structure has essentially converged. The correlation function is reproduced to a good precision. The remaining discrepancies are due to the fact that the correlation function in Eq. (13) is not physically realizable in the case of complete segregation [25]. Several necessary conditions for realizability, in addition to the ones discussed by Torquato [26], will be reported in a forthcoming publication. For reasonable choices of the parameters, however, stochastic minimization will still find a structure that approximates Eq. (13) to a satisfactory precision. Although a much smaller resolution would have been sufficient in this case, 1024×1024 pixels have been used for consistency with the following example.

In order to illustrate the additional capabilities offered by the algorithm, Fig. 4(e) shows a similar structure calculated for the correlation function

$$G(\mathbf{r}) = \phi^2 + \frac{1}{2}\phi(1-\phi)e^{-r/r_0}\left[\frac{\sin(2\pi r/a_0)}{2\pi r/a_0} + \frac{\sin(2\pi r/a_1)}{2\pi r/a_1}\right], \qquad (14)$$

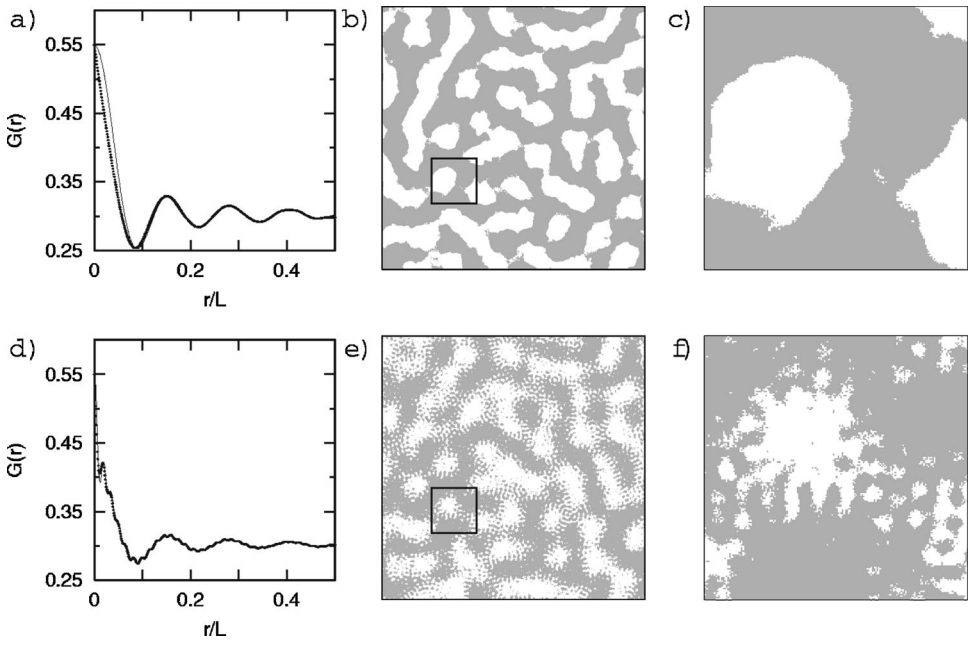

FIG. 4. Construction of two-phase structures from the analytically given correlation functions shown by solid lines in (a) [Eq. (13)] and (d) [Eq. (14)]. L is the linear size of the periodic cell. The target correlation function (a) contains one structural length scale, whereas (d) includes additional short-range oscillations. (b) and (e) show the resulting structures on a 1024×1024 grid after 9 000 000 attempted Monte Carlo moves. The correlation functions corresponding to the structures (b) and (e) are shown as dotted lines in (a) and (d), respectively. Magnifications of the indicated regions are shown in (c) and (f).

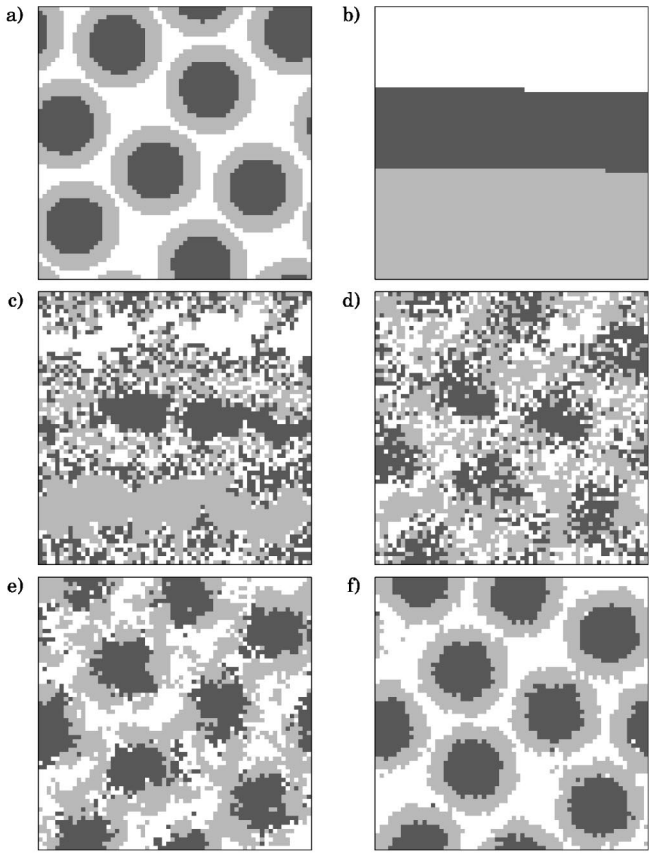

FIG. 5. Reconstruction of a triphase core-shell structure. (a) Target system, (b) initial configuration, (c) configuration after 3427 attempted Monte Carlo moves (2000 accepted steps), (d) configuration after 9501 attempted Monte Carlo moves (4000 accepted steps), (e) configuration after 25 176 attempted Monte Carlo moves (6000 accepted steps), (f) final configuration (200 000 attempted Monte Carlo moves, 7771 accepted steps).

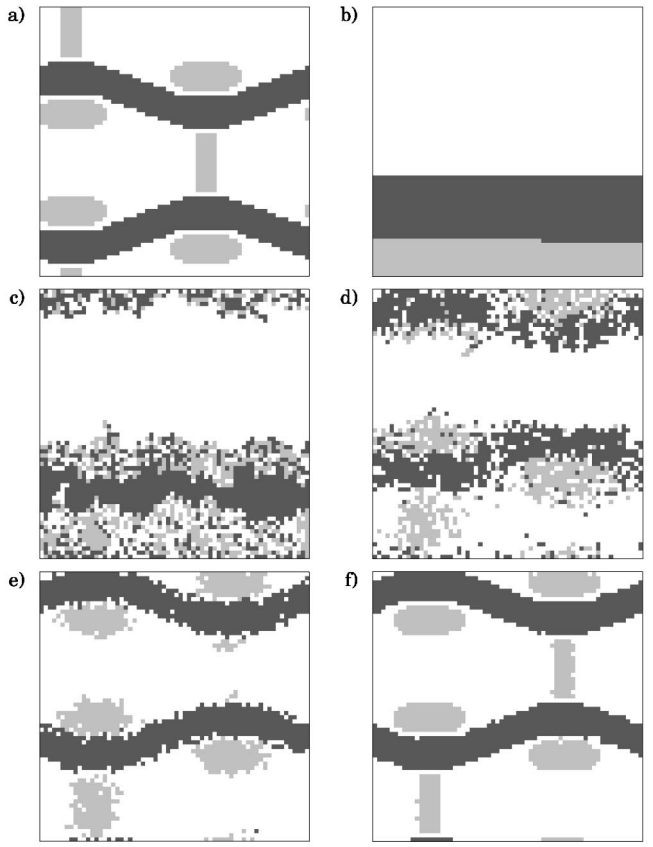

FIG. 6. Reconstruction of a triphase knitted structure analogous to a triblock copolymer system [29]. (a) Target system, (b) initial configuration, (c) configuration after 1684 attempted Monte Carlo moves (1000 accepted steps), (d) configuration after 8446 attempted Monte Carlo moves (3000 accepted steps), (e) configuration after 16 713 attempted Monte Carlo moves (4000 accepted steps), (f) final configuration (200 000 attempted Monte Carlo moves, 4519 accepted steps).

with $a_1 = 0.0125L$. All other parameters have the same values as in the previous example. This system has *two different* structural length scales given by a_0 and a_1. Such structures must be represented by a highly resolved grid (1024×1024 in this case). Whereas the computational demands would have been close to prohibitive for previously proposed algorithms, the calculation converged after about 24 h of CPU time on 8 nodes of a parallel workstation cluster using the method presented here.

C. Triphase systems

Many important materials consist of more than two phases. Therefore, the new algorithm has been implemented to deal with multiphase systems. This capability, which requires the consideration of autocorrelation as well as cross-correlation functions, is illustrated below using example structures that have been selected in analogy to some of the microstructures observed in triblock copolymers. This class of materials is well known to phase separate into a rich variety of microstructures depending on the relative length of the different blocks [27,28].

Figure 5 shows an example of the reconstruction of a hypothetical periodic particulate system of disks of phase *A* enclosing a ''nucleus'' of phase *B*, interspersed in a matrix *C*. Volume fractions are $\phi_A = 0.4$, $\phi_B = 0.3$, and $\phi_C = 0.3$. The target configuration [Fig. 5(a)] was obtained using Monte Carlo mixing of hard disks and subsequent digitization on a 64×64 grid. Figures 5(c), 5(d), 5(e), and 5(f) show the reconstructed system after 3427, 9501, 25 176, and 200 000 attempted Monte Carlo moves, respectively.

A second example is presented in Fig. 6. It corresponds to a two-dimensional section through a periodic 3D layerlike structure, which has been observed experimentally in a triblock copolymer [29]. The periodic cell of the microstructure was digitized on a 64×64 grid.

The CPU time necessary for reconstructions was ≈ 98 sec for both examples. The computations were performed on an AMD K7 700 MHz based computer.

IV. PARALLELIZATION

The proposed algorithm is ideally suited for parallel distributed-memory machines. In our implementation each

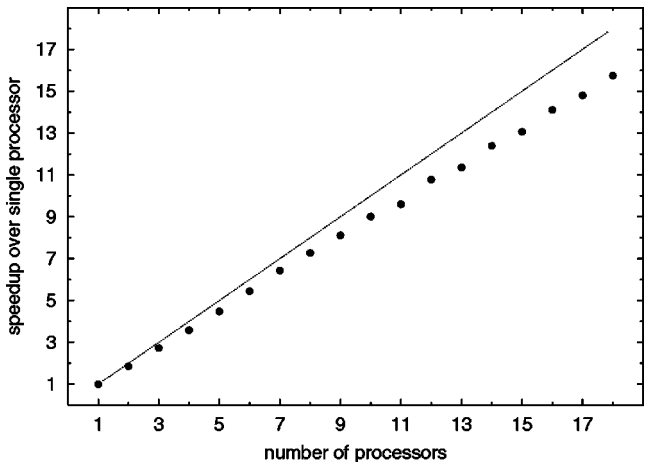

FIG. 7. Scaling of the algorithm on a cluster of Pentium III 500 MHz machines with 100 Mbit/sec Ethernet communications.

computational node is responsible for a slice of the correlation functions. One node acts as a master, selecting a pair of pixels for Monte Carlo exchange and broadcasting it to the slaves. These then update their slices of the correlation functions according to Eqs. (A5)–(A8) and report the respective contributions to the discrepancy back to the master. To this effect, it is necessary for each slave to store the entire current configuration as well as the relevant slices of the target correlation functions. The master then decides whether or not to accept the move and broadcasts its decision to the slaves, which in turn update the locally stored current configuration. The communication load generated by this scheme is minimal; at each cycle only a few integer numbers for the candidate pixel positions, the discrepancy, and the acceptance decision need to be exchanged between master and slaves. This represents another advantage over Fourier transform methods, since parallelization of the FFT algorithm generates a much larger communication load [30, Chap. 3].

Figure 7 shows the speedup of the algorithm as a function of the number of processors for a two-phase system on a 3072×3072 grid. The scaling is linear over the entire range and no saturation effects are observable.

V. CONCLUSIONS

A highly efficient Monte Carlo minimization algorithm for the reconstruction of multiphase microstructures from correlation functions has been introduced. The method computes the response of the correlation functions to *localized* changes in the underlying densities. This decreases the CPU time per Monte Carlo step by one to two orders of magnitude compared to previous methods [13]. In addition, candidates for Monte Carlo moves are selected exclusively at phase boundaries, leading to a greatly enhanced rate of convergence. The two improvements are independent from each other. Their effect on the overall CPU time needed for restoration is multiplicative.

The speedup is such that problems that were previously out of reach due to the computational demand can now be treated. This includes systems that require high resolution due to the presence of several structural length scales as well as multiphase systems, where more than one correlation function is relevant.

An interactive demonstration of the method as well as animated versions of Figs. 2, 5, and 6 are available on the authors' web site [31].

ACKNOWLEDGMENTS

The authors are grateful to Professor R. Jones, Department of Physics, University of Connecticut for providing access to his workstation cluster for the scaling experiments. M.G.R. acknowledges partial support from the Estonian Science Foundation under the Grant No. 4032.

APPENDIX: IMPLEMENTATION OF THE UPDATE PROCEDURE

In the following, detailed formulas are given for the update of correlation functions after exchange of the contents of two pixels. These formulas are essentially discretized versions of the fundamental relationship given in Eq. (9), and can directly be used in order to implement the algorithm on a computer. In the following $\mathbf{r}$, $\mathbf{a}$, and $\mathbf{b}$ denote vectors on the discrete grid of an arbitrary number of dimensions. It is advantageous to work with un-normalized discrete representations of the correlation functions defined as

$$G_{ij}(\mathbf{r})=\sum_{\mathbf{r}'}\rho_i(\mathbf{r}')\rho_j(\mathbf{r}+\mathbf{r}'). \tag{A1}$$

Consider two pixels located at the grid points $\mathbf{a}$ and $\mathbf{b}$. Assume them to contain components i and j, respectively. If the contents of those two pixels are exchanged, the density functions ρ_i and ρ_j transform in the following way:

$$\rho_i(\mathbf{r})\rightarrow\rho_i(\mathbf{r})-\delta(\mathbf{r}-\mathbf{a})+\delta(\mathbf{r}-\mathbf{b}), \tag{A2}$$

$$\rho_j(\mathbf{r})\rightarrow\rho_j(\mathbf{r})+\delta(\mathbf{r}-\mathbf{a})-\delta(\mathbf{r}-\mathbf{b}). \tag{A3}$$

Here, $\delta(\mathbf{r})$ has the meaning of the Kronecker tensor; it is unity if all components of its argument vanish and zero otherwise. All other density functions are, of course, unaffected by the move, hence

$$\rho_k(\mathbf{r})\rightarrow\rho_k(\mathbf{r}),\quad k\neq i,j. \tag{A4}$$

Four different cases must be discussed for the update of the discretized correlation functions. Trivially, correlation functions that involve neither of the two components i and j remain unaffected,

$$G_{lm}(\mathbf{r})\rightarrow G_{lm}(\mathbf{r}),\quad l,m\neq i,j. \tag{A5}$$

Correlation functions involving exactly one of the two components i and j transform as

$$G_{im}(\mathbf{r})\rightarrow G_{im}(\mathbf{r})-\rho_m(\mathbf{r}+\mathbf{a})+\rho_m(\mathbf{r}+\mathbf{b}),\quad m\neq j, \tag{A6}$$

whereas the cross-correlation function between i and j must be updated as

$$G_{ij}(\mathbf{r}) \to G_{ij}(\mathbf{r}) + \rho_i(\mathbf{a}-\mathbf{r}) - \rho_i(\mathbf{b}-\mathbf{r}) - \rho_j(\mathbf{a}+\mathbf{r}) + \rho_j(\mathbf{b}+\mathbf{r}) + \delta(\mathbf{b}-\mathbf{a}-\mathbf{r}) + \delta(\mathbf{a}-\mathbf{b}-\mathbf{r}) - 2\delta(\mathbf{r}). \quad \text{(A7)}$$

Finally the autocorrelation functions G_{ii} and G_{jj} transform as follows:

$$G_{ii}(\mathbf{r}) \to G_{ii}(\mathbf{r}) - \rho_i(\mathbf{a}-\mathbf{r}) + \rho_i(\mathbf{b}-\mathbf{r}) - \rho_i(\mathbf{a}+\mathbf{r}) + \rho_i(\mathbf{b}+\mathbf{r}) - \delta(\mathbf{a}-\mathbf{b}+\mathbf{r}) - \delta(\mathbf{b}-\mathbf{a}+\mathbf{r}) + 2\delta(\mathbf{r}), \quad \text{(A8)}$$

$$G_{jj}(\mathbf{r}) \to G_{jj}(\mathbf{r}) + \rho_j(\mathbf{a}-\mathbf{r}) - \rho_j(\mathbf{b}-\mathbf{r}) + \rho_j(\mathbf{a}+\mathbf{r}) - \rho_j(\mathbf{b}+\mathbf{r}) - \delta(\mathbf{a}-\mathbf{b}+\mathbf{r}) - \delta(\mathbf{b}-\mathbf{a}+\mathbf{r}) + 2\delta(\mathbf{r}). \quad \text{(A9)}$$

Note that Eqs. (A5)–(A8) conserve the normalization of the correlation functions, i.e., $G_{ij}(0) \to G_{ij}(0)$ for all i,j.

As is evident from these update formulas, the entire Monte Carlo algorithm, including the calculation of the discrepancy, involves only addition and multiplication operations and never division. This is important, since it makes it possible to implement the algorithm entirely in terms of integer numbers. Depending on the computer architecture used, this may bring about another speed advantage. Even more importantly, it completely removes any accumulation of roundoff errors. Given a fully representable set of discretized correlation functions, the algorithm is thus capable of providing an *exact* solution.

[1] J. W. Cahn, J. Chem. Phys. **42**, 93 (1965).
[2] J. A. Quiblier, J. Colloid Interface Sci. **98**, 84 (1984).
[3] N. F. Berk, Phys. Rev. Lett. **58**, 2718 (1987).
[4] N. F. Berk, Phys. Rev. A **44**, 5069 (1991).
[5] M. Teubner, Europhys. Lett. **14**, 403 (1991).
[6] A. P. Roberts and M. Teubner, Phys. Rev. E **51**, 4141 (1995).
[7] A. P. Roberts, Phys. Rev. E **56**, 3203 (1997).
[8] A. P. Roberts and S. Torquato, Phys. Rev. E **59**, 4953 (1999).
[9] P. M. Adler, *Porous Media: Geometry and Transport* (Butterworth-Heinemann, Boston, 1992).
[10] P. Levitz, Adv. Colloid Interface Sci. **76-77**, 71 (1998).
[11] C. L. Y. Yeong and S. Torquato, Phys. Rev. E **57**, 495 (1998).
[12] C. L. Y. Yeong and S. Torquato, Phys. Rev. E **58**, 224 (1998).
[13] D. Cule and S. Torquato, J. Appl. Phys. **86**, 3428 (1999).
[14] C. Manwart and R. Hilfer, Phys. Rev. E **59**, 5596 (1999).
[15] C. Manwart, S. Torquato, and R. Hilfer, Phys. Rev. E **62**, 893 (2000).
[16] D. Choy and S.-H. Chen, Phys. Rev. E **61**, 4148 (2000).
[17] H. Jinnai *et al.*, Phys. Rev. E **61**, 6773 (2000).
[18] N. Losic, J.-F. Thovert, and P. M. Adler, J. Colloid Interface Sci. **186**, 420 (1997).
[19] J. Bernasconi, J. Phys. (Paris) **48**, 559 (1987).
[20] W. Krauth and O. Pluchery, J. Phys. A **27**, L715 (1994).
[21] W. Krauth and M. Mezard, Z. Phys. B: Condens. Matter **97**, 127 (1995).
[22] W. Wenzel and K. Hamacher, Phys. Rev. Lett. **82**, 3003 (1999).
[23] Equation (5) is tacitly understood to be averaged over a small region of space around **r**. In this way, the density and the correlation functions always remain finite and bounded, in spite of the singularity introduced by the δ function.
[24] M. Frigo and S. G. Johnson, in *Proceedings of the 1998 IEEE International Conference on Acoustics, Speech, and Signal Processing, ICASSP98* (IEEE, New York, 1998), Vol. 3, pp. 1381–1384 (the FFT library and documentation are available from http://www.fftw.org).
[25] In the case of complete segregation, i.e., when the characteristic density functions $\rho_i = 0,1$ [cf. Eqs. (11) and (12)], the second derivative of the correlation function vanishes at the origin, $G''(0) \equiv 0$ [see R. Kirste and G. Porod, Kolloid Z. Z. Polym. **184**, 1 (1962)]. This condition is violated by Eqs. (13) and (14).
[26] S. Torquato, J. Chem. Phys. **111**, 8832 (1999).
[27] I. W. Hamley, *The Physics of Block Copolymers* (Oxford University Press, Oxford, 1998).
[28] F. S. Bates and G. H. Fredrickson, Phys. Today **52**, 32 (1999).
[29] U. Breiner, U. Krappe, E. L. Thomas, and R. Stadler, Macromolecules **31**, 135 (1998).
[30] C. Van Loan, *Computational Frameworks for the Fast Fourier Transform* (SIAM, Philadelphia, 1992).
[31] http://giotto.ims.uconn.edu/.